BENDING PROPERTIES OF HIGH PERFORMANCE CARBON FIBER REINFORCED CONCRETE BEAMS

W. I. Khalil[1], A. A. Mahmood[2]

Abstract

The flexural behavior of high performance reinforced concrete beams containing chopped carbon fibers with different volume fractions (0%, 0.2%, 0.3%, 0.4% and 0.5%) in full and partial depths of beams cross sections is studied in this investigation. The load deflection relationship, resilience, toughness indices, first crack and ultimate loads, concrete and steel strains were investigated. Generally, the experimental results show that the fiber volume fraction has no significant effect on load-deflection and ultimate load of beam specimens, while, it has a considerable effect on the first crack load, resilience and toughness indices. The ultimate strength of fibre reinforced concrete (FRC) has been rederived and contributed in order to calculate the moment capacity of high performance carbon fiber concrete beams. The calculated ultimate moment capacity was in good agreement with the measured ultimate moment capacity. The results also show that applying the conventional flexural theory ACI 318 and ACI 544 model cause significant error in estimating the moment capacity of carbon fiber reinforced concrete beams.
Keywords: high performance, carbon fiber, volume fraction, ultimate strength

1. Introduction

The high compressive strength of high performance concrete (HPC) can be used advantageously in compression members such as columns and piles. The relatively higher compressive strength per unit volume and per unit weight will also significantly reduce the dead load of flexural members. In addition, HPC possessing a highly dense microstructure is likely to enhance long-term durability of the structure. Producing HPC requires more care in preparing, mixing, compacting and placing than normal concrete [1]. HPC is considered as a relatively brittle material so using discontinues fibers enhance it's ductility. When concrete cracks, the randomly oriented fibers start functioning, arresting both the randomly oriented micro-cracking and its propagation and thus improving strength and ductility [2]. If property designed, fibers can be added to structural member especially when used together with conventional steel main reinforcements (rebar) [3]. Little work has been done to investigate the mechanical properties of normal strength carbon fiber concrete [4,5]

[1] Wasan I. Khalil, University of Technology-Building&Construction Department, Bagdad, Iraq, wasan1959@yahoo.com

[2] Akar Abdulrazzaq Mahmood, M.Sc. in structural Engineering-Halabja Group-Sulaimaniyah, Iraq, akar.razzaq@halabjagroup.com

and mechanical properties of HPCFC[6], no detailed studies are found on the structural behavior of HPCFC beams.

2. Experimental Work

2.1 Materials

Ordinary Portland cement with physical and chemical properties conform to the provisions of Iraqi specification No. 5/1984, local natural sand it's gradation lays in zone (2) according to Iraqi specification No. 45/1984, local normal weight crushed aggregate of maximum size 12.5mm it's grading conforms to the Iraqi specification No. 45/1984 were used in this investigation. High range water reducing admixture (HRWRA) chemicaly it is Naphthalene Formaldehyde Sulphonate, Which is known commercially as Sikament-FFN was also used, it is (HRWRA) type F according to ASTM C 494 specifications. The reduction in water content was determined in order to obtain a constant workability with slump 85±5 mm. Condensed silica fume was used as pozzolanic admixture, it's physical requirement, pozzolanic activity index and chemical oxide compositions conform to the requirements of ASTM C 1240-05 specifications.
Grade 60 ordinary deformed mild-steel reinforcing bars with two different diameters (12 and 8mm) are used as reinforcement in this investigation. The dimensions and strength characteristics of these bars are summarized in Table (1). The stress-strain curves for 12 and 8 mm reinforcing steel bars have been drawn to be used in the calculations as shown in Fig.(1) . High strength chopped carbon fiber (CF) was also used in this investigation with filament diameter 7 μmm, filament length 5-6mm, tensile strength 3450 MPa , tensile modulus of elasticity 230 GPa, elongation 1.5%, specific gravity 1.8 and carbon content 98%.

Table 1: Properties of main bars and stirrups reinforcement *

Reinforcing steel bars	Diameter (mm)	Area (mm^2)	Yield Strength (MPa)	Tensile Strength (MPa)	ASTM A 615-05 Specification		Modulus of Elasticity (GPa)	Elongation (%)
					Min. Yield St. (MPa)	Max. Tensile Str. (MPa)		
Tension bars	12.0	113.1	490	760	420	620	184	18.1
Compression bars & stirrups	8.0	50.3	637	757	-----	-----	194	15.2

*Note: The results are the average for three bar specimens.

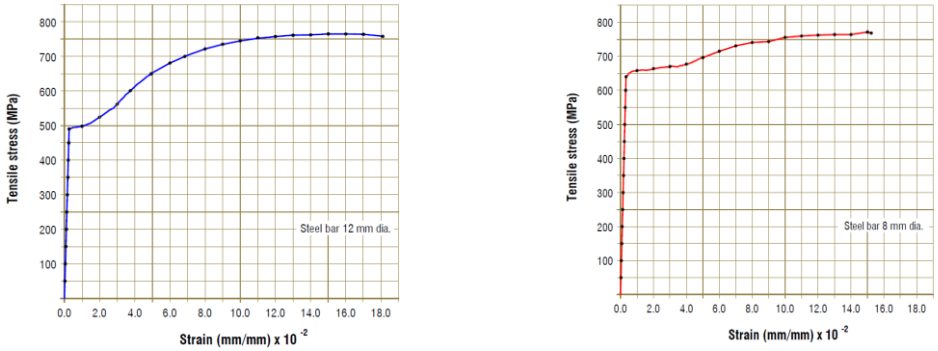

Fig.1: stress-strain curve for reinforcing steel bars

2.2 Concrete Mixes and Mixing Procedure

Several trial mixes were carried out in previous research [6] to produce HPC mix. One mix was selected to manufacture the conventional steel reinforced beam containing CF with different volume fractions (0.2%, 0.3%, 0.4% and 0.5%) in full and partial depths of beams cross sections. The mix proportions is 1:1.19:1.8 by weight (cement: sand: aggregate), water/cementations ratio 0.33, HRWRA with 3 % dosage by weight of cement and silica fumes dosage 15 % by weight of cement as addition of cement content. The compressive strength was 78.8 MPa at 28 days. For non-fibrous concrete mix, coarse aggregate, some of the mixing water and the solution of admixture (when required) were placed in the mixer and mixed for about 1 min. After that, fine aggregate, cement, silica fume and the remaining water were loaded to the mixer and mixed for about 5 min. For CF concrete mix, water, aggregate and cement have been fully mixed then fibers were slowly added to the concrete by hand spraying, while the mix was rotating and mixed for 3 min.

2.3 Preparation of Specimens

Concrete beam specimen was casted in steel mould with internal dimensions of 150 x 300 x 2000 mm. The beam specimens were designed according to the appropriate ACI 318M-08 design code [7], they were doubly reinforced in the tension and compression zones, for each beam specimens two electrical strain gauges were bonded at each tensile and compressive reinforcing steel bars as shown in Fig.(2). The beams were cast in three layers and sufficient internal vibration has been applied to each layer. In partial depth FRC beams, a layer of FRC was placed first and compacted, then the process was repeated until the required depth of FRC had been placed. Thereafter, the remaining portion of the plain concrete was placed and compacted. Control specimens were prepared from the same mix of plain and FRC for each beam specimen, they were compacted by using external vibrating table. These specimens include compressive strength concrete cubes of 100 mm, concrete cylinders of 150 x 300 mm for splitting tensile strength and static modulus of elasticity tests, and concrete prisms of 100 x 100 x 500 mm for modulus of rupture test. After demoulding the beams and control specimens, curing process was done by covering the specimens with wet burlap and spraying water on them every day, then covering them with polyethylene sheets and a blanket to ensure full saturated humidity state. The

specimens were cured for 28 days after that they were kept in laboratory to be normally air dried until the time of testing.

2.4 Test Variables and Flexural Strength Test of Beams

Test specimens were classified to four series. The main test variables were volume fraction (V_f) of CF and depth of fiber inclusion in the beams as shown in Table (2). The beams were tested under a four-point loading system. They were simply supported on 1800mm span and two concentrated loads (500mm spacing) were applied at 650mm from each supports. The locations of dail gauge used to measure the deflection, demec points for a 150mm mechanical extensometer and electrical strain gauges are shown in Fig.(2).

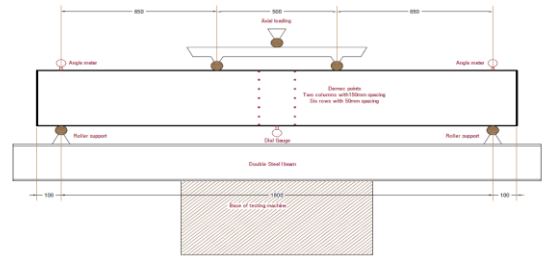

(A)

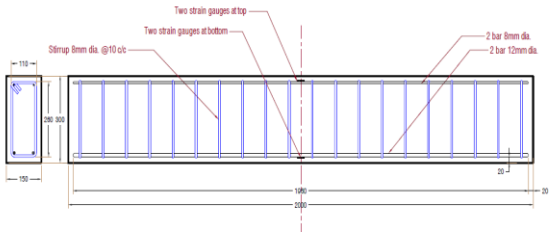

(B)

Fig2: A-Flexural test set-up for beam specimens
B-Typical concrete beam specimen dimensions and reinforcing steel bars (unit:mm)

Table 2: Details of tested beam specimens

Test series	beam label	V_f (%)	Depth of fiber inclusion
1	$D_{300}V_{0.0}$	0.00	---
2	$D_{300}V_{0.2}$	0.20	Full depth (300 mm)
	$D_{300}V_{0.3}$	0.30	Full depth (300 mm)
	$D_{300}V_{0.4}$	0.40	Full depth (300 mm)
	$D_{300}V_{0.5}$	0.50	Full depth (300 mm)
3	$D_{150}V_{0.2}$	0.20	1/2 depth (150 mm)
	$D_{150}V_{0.3}$	0.30	1/2 depth (150 mm)
	$D_{150}V_{0.4}$	0.40	1/2 depth (150 mm)
	$D_{150}V_{0.5}$	0.50	1/2 depth (150 mm)
4	$D_{100}V_{0.2}$	0.20	1/3 depth (100 mm)
	$D_{100}V_{0.3}$	0.30	1/3 depth (100 mm)
	$D_{100}V_{0.4}$	0.40	1/3 depth (100 mm)
	$D_{100}V_{0.5}$	0.50	1/3 depth (100 mm)

3. Experimental Results and Discussion

3.1 Load –Deflection Relationship

The effect of different volume fractions of CF in full, half and one-third depth of reinforced concrete beam specimens on load-deflection relationship are shown in Figures (3), (4) and (5) respectively. Generally a relatively stiffer response can be observed at the post-cracking stage for all beam specimens containing CF. This may be due to the high

specific strength and stiffness of CF [8,9]. It can also be seen that CF cause a desire modification in the deformational characteristics of conventional reinforced HPC beams subjected to pure bending for almost the entire range of loading (from first crack to ultimate load). Both first crack and ultimate flexural loads increase, while the deflection of a particular load level decreases relative to the reference beam specimen (without CF). For the range of service loads, such modifications are more significant and desirable since they result in less crack width, reduction in deflection and higher flexural rigidity. This improvement may be attributed to the high bond between fibers and matrix which is achieved with densification of the matrix by silica fume combined with a low water/cement ratio [10], and the behavior of fibers as crack bridging which made fiber reinforced concrete capable to carry the load well after the development of crack on the concrete [2, 9, 11]. The results also indicate that the fiber volume fraction has no significant effect on the load-deflection pattern of beam specimens. Figures (6) to (9) show the load-deflection curves for full and partial depth fiber reinforced high performance concrete beam specimens. Generally it is clear that for a specific volume fraction of fiber, the load-deflection patterns for specimens with partial depth fiber inclusion are similar to those of the corresponding full depth fiber reinforced beams, especially for volume fractions of 0.3% and 0.5% as shown in Figures (7) and (9) respectively. It can be concluded that partial depth inclusion of fiber can be used in more efficient and economical manner. Other researchers [12, 13] who investigated the effect of inclusion steel fiber on the structural behavior of concrete specimens have reported similar results.

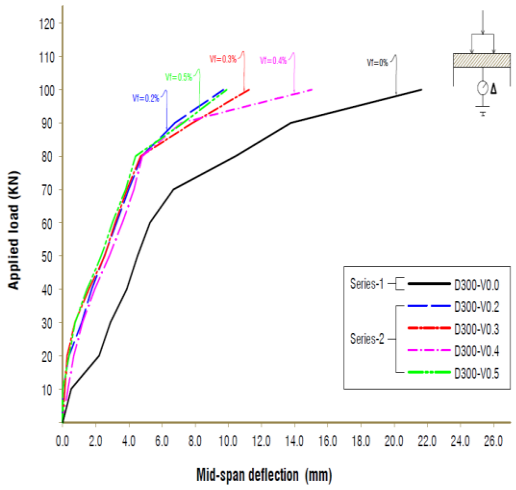

*Fig.3:*Load-deflection relationship at mid-span of full depth FRC beam specimens (series1&2)

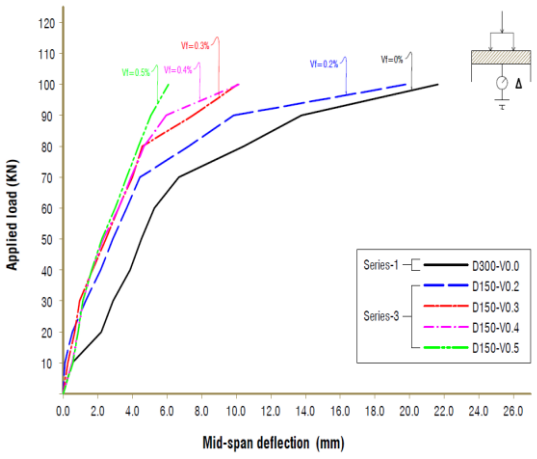

*Fig.4:*Load-deflection relatioship at mid-span of half depth FRC beam specimens (series1&3)

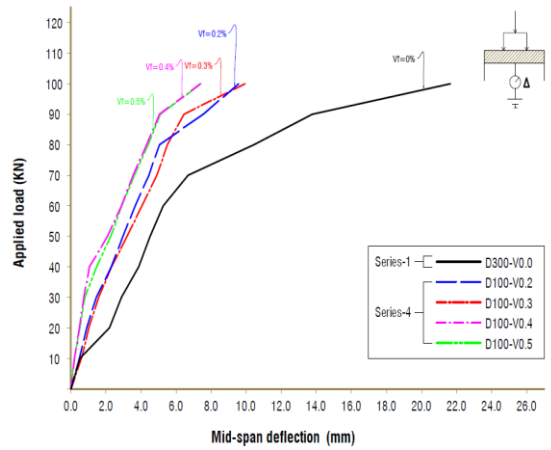

*Fig.5:*Load-deflection relationship at mid-span of one-third depth FRC beam specimens (series1&4)

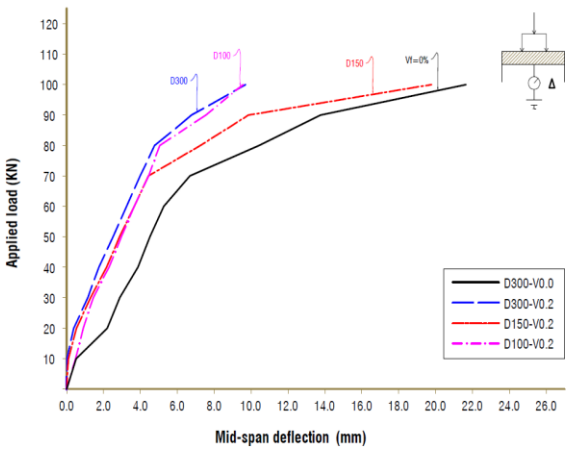

*Fig.6:*Load-deflection relatioship at mid-span of various fiber depth inclusion beam specimens with V_f 0.2%

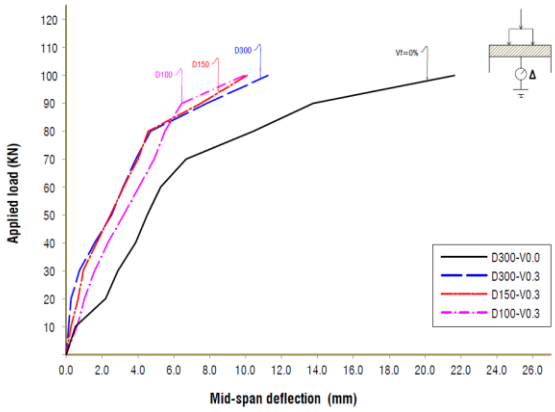

*Fig.7:*Load-deflection relationship at mid-span of various fiber depth inclusion beam specimens with V_f 0.3%

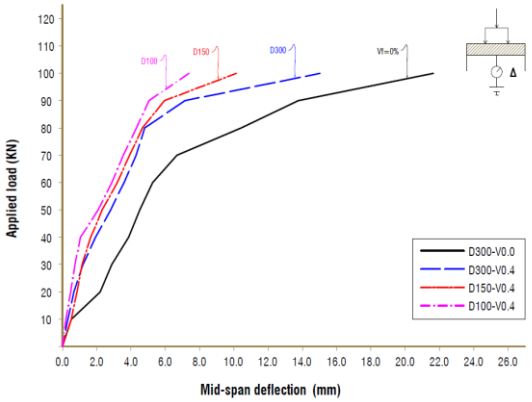

*Fig.8:*Load-deflection relatioship at mid-span of various fiber depth inclusion beam specimens with V_f 0.4%

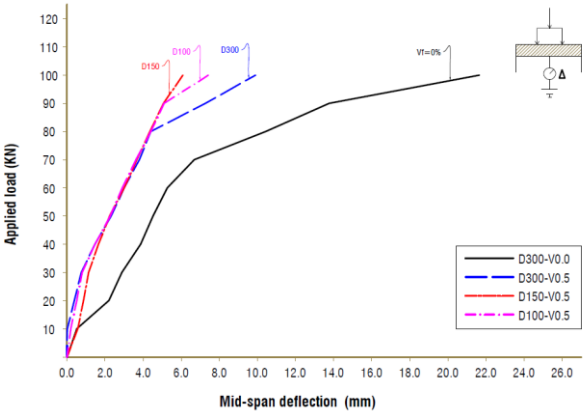

*Fig.9:*Load-deflection relatioship at mid-span of various fiber depth inclusion beam specimen with V_f 0.5%

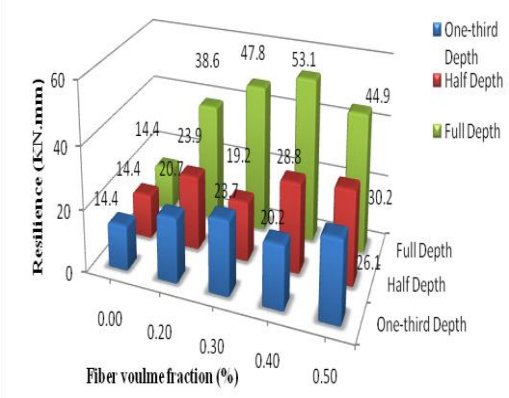

Fig.10: Comparison of resilience of beam specimens

3.2 First Crack and Ultimate Loads and Moments

First crack and ultimate loads and moments results of the FRC beams are shown in Table (3). The results indicate that the addition of CF causes a considerable increase in the first crack load; the percentage increase for full depth fiber inclusion is between 80-105%, while there is a slight increase in ultimate load between 7-14% relative to the plain concrete beam. The considerable increase in first crack load for FRC beam specimens is attributed to the stress transfer capability of the reinforcing fibers, which leads to stress redistribution to occur, so the localized fracture will be delayed. As the cracks developed in the fracture region due to the increase in loads, the contribution of fibers in the flexural region declined. [14]

3.3 Resilience

Figure (10) shows the effect of CF volume fraction and the depth of fiber inclusion on the resilience of beam specimens. Generally it is noted that the resilience of CF beam specimens significantly increases in comparison with the reference beam specimen, also the resilience increases as fiber volume fraction increases. Also it can be seen that the resilience of beam specimens with full depth fiber inclusion is significantly increase relative to reference beam specimen, while the increase for beams with partial depth fiber inclusion is less than that with full depth fiber inclusion. The percentage increase for beams with full depth fiber inclusion is about 169%, 233%, 270% and 213%, while the percentage increase for beams with one-third fiber depth is about 44%, 65, 40% and 81% for fiber volume fractions 0.2%, 0.3%, 0.4% and 0.5% respectively.

Table 3: First crack and ultimate loads and moments results for tested beam specimens

Test series	Test beam label	Applied load ($P_{exp.}$)		Increment in load with respect to Beam $D_{300}V_{0.0}$		Applied moment ($M_{exp.}$)	
		First crack load (KN)	Failure load (KN)	First cracking %	Failure load %	First crack moment P/2 x 0.65 (KN.m)	Failure moment P/2 x 0.65 (KN.m)
1	$D_{300}V_{0.0}$	20	118			6.50	38.35
	$D_{300}V_{0.2}$	37	132	85.0	11.9	12.03	42.90
	$D_{300}V_{0.3}$	41	127	105.0	7.6	13.33	41.28
	$D_{300}V_{0.4}$	36	126	80.0	6.8	11.70	40.95
2	$D_{300}V_{0.5}$	38	134	90.0	13.6	12.35	43.55
	$D_{150}V_{0.2}$	29	119	45.0	0.8	9.43	38.68
	$D_{150}V_{0.3}$	35	128	75.0	8.5	11.38	41.60
	$D_{150}V_{0.4}$	38	131	90.0	11.0	12.35	42.58
3	$D_{150}V_{0.5}$	39	135	95.0	14.4	12.68	43.88
	$D_{100}V_{0.2}$	29	134	45.0	13.6	9.43	43.55
	$D_{100}V_{0.3}$	26	125	30.0	5.9	8.45	40.63
	$D_{100}V_{0.4}$	42	130	110.0	10.2	13.65	42.25
4	$D_{100}V_{0.5}$	38	133	90.0	12.7	12.35	43.23

3.4 Toughness Indices Results

The toughness index values were calculated by using ASTM C1018 method. The areas under the load-deflection curve up to the first crack deflection and at selected multiples of first deflection of reinforced concrete beams were calculated by Auto CAD software computer program. The values of toughness indices of all tested beam specimens have been presented in Figures (11) and (12). Generally, it can be seen that the toughness of all FRC beam specimens is considerably enhanced over that of plain concrete beam specimen. In case of fully depth CF reinforced beam specimens, the values of indices I_5 and I_{10} are higher than the standard values 5 and 10 respectively. This indicates that up to 5.5 times of the cracking deflection, the post-cracking performance of these specimens is better than the elastic-plastic behavior and the load carrying is increased beyond that of matrix cracking, the values of indices I_5 and I_{10} for partial depth FRC beam specimens are higher than that for full depth FRC beam specimens. Beam specimens with one-third fiber depth inclusion and volume fraction of 0.2% and 0.3% show optimum toughness index values, the values of I_5 are 6.4 and 24.8, while the values of I_{10} are 7.1 and 29.3 respectively. This enhanced performance of fiber reinforced beam specimens results from their improved capacity to absorb energy during fracture since fibers continue to carry stresses beyond matrix cracking, and this helps to maintain structural integrity and cohesiveness in the material [9, 11, 14].

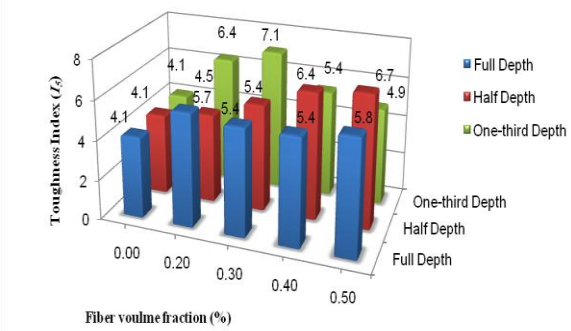

Fig.11: Comparison of toughness index (I_5) of beam specimens

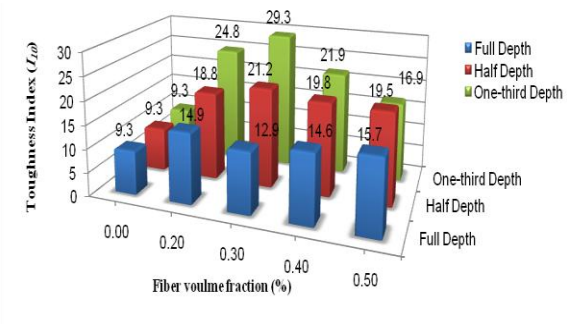

***Fig**. 12:* Comparison of toughness index (I_{10}) of beam specimens

3.5 Concrete Strains for Beam Specimens

The concrete strains were measured at each load step during the flexural test of beam specimens. Figures (13) to (15) show the strains variation diagram at the mid-span cross section for beam specimens containing various fiber volume fractions with full, half and one-third fiber depth inclusions respectively. The strains readings were more difficult beyond 100 KN load due to continuous change in strains up to failure load. There is a significant difference in strains between the FRC beams and non-FRC beams. This difference is most likely explained by a structural effect (neutral axis position and section equilibrium) combined with a modification of the material behavior in the tensile part of the beams due to the short CF reinforced concrete [15]. Generally, the depth of neutral axis (measured from extreme compression fiber), tensile strain and compressive strain for all

FRC beams were reduced compared with non-FRC beam. Full and partial depth fiber inclusions have a slight effect on the strains, except for beam $D_{150}V_{0.2}$.

3.6 Steel Bars Strains for Beam Specimens

Figures (16) to (18) represent the average strain evolution of the upper and lower reinforcing bars due to the applied load during the flexural test of beam specimens. The load-strain curves illustrate the behavior per unit length up to the yield point for the tension steel bars. From these results the yield load is determined by substituting the tension yield strain 0.00266 (ratio of yield strength / modulus of elasticity) for beams during the loading stage, so the yield load and yield moment of beam specimens are shown in Table (4). From these results it can be noted that the yield load in the steel bars for FRC beams is higher than that for plain concrete beam. This is attributed to the enhancement of the bond strength between steel bars and the matrix around the bar, due to the addition of CF and silica fume to the concrete. This leads to more ductile and stable pull-out bars, which in turn contributes to the ductile behavior of the entire structural member [14].

3.7 Failure Modes for Beam Specimens

All the beams failure was due to yielding of deformed tensile reinforcing steel bars as shown in Table (5) and spalling of concrete on the compressive side, the compression reinforcing bars did not yield when the doubly reinforced beam failed in flexure. The buckling of compression reinforcing bars did not occur due to nominal ties at spacing of 100mm. At the load of failure the compression and tension strains in reinforcing steel bars were recorded as presented in Table (5). The strain for each reinforced bars was converted to stress by using strain-stress diagram of reinforced steel bars shown in Fig.(1).

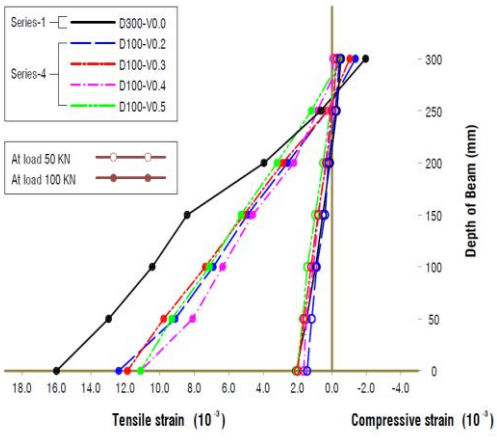

Fig.13: Strain diagram in mid-span cross section of full depth FRC beams (series1&2)

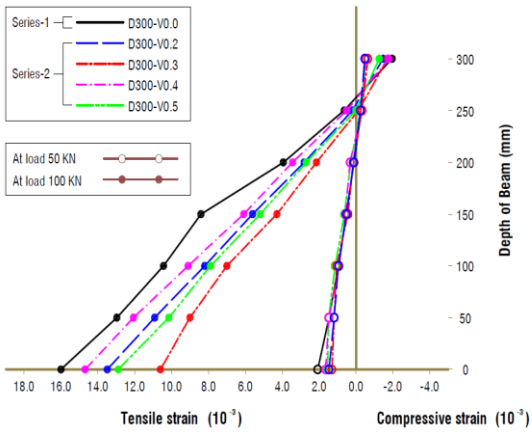

Fig.14: Strain diagram in mid-span cross section of half depth FRC beams (series1&3)

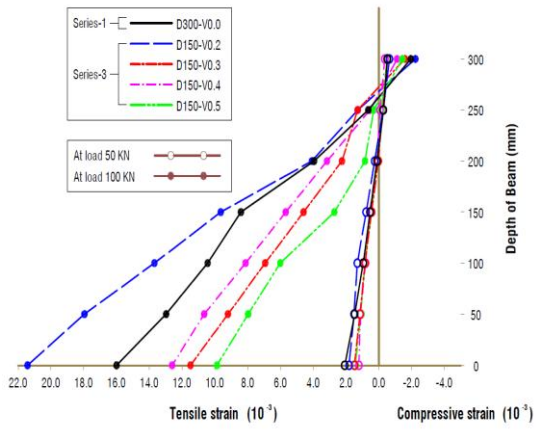

*Fig.15:*Strain diagram in mid-span cross section of one-third depth FRC beams (series1&4)

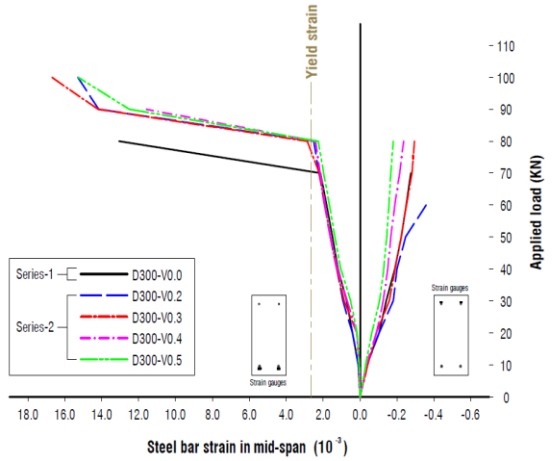

*Fig.16:*Steel bar strain at mid-span of full depth FRC beams (series1&2)

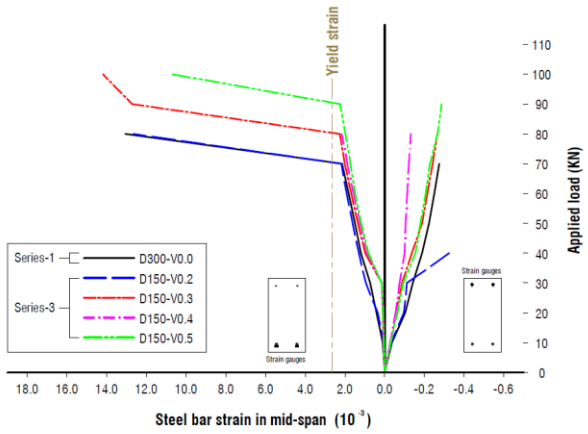

*Fig.17:*Steel bar strain at mid-span of half depth FRC beams (series1&3)

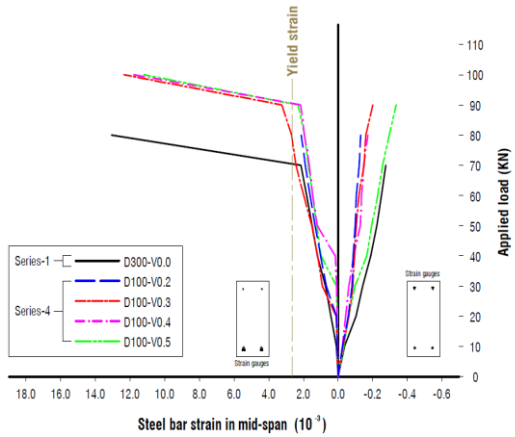

*Fig.18:*Steel bar strain at mid-span of one-third depth FRC beams (series1&4)

Table 4: Yield load and yield moment results for beam specimens

Test series	Test beam label	Yield load (KN)	Yield Moment (KN.m)
1	$D_{300}V_{0.0}$	70.5	22.9
2	$D_{300}V_{0.2}$	78.9	25.6
	$D_{300}V_{0.3}$	76.9	25.0
	$D_{300}V_{0.4}$	78.3	25.4
	$D_{300}V_{0.5}$	80.4	26.1
3	$D_{150}V_{0.2}$	70.5	22.9
	$D_{150}V_{0.3}$	76.4	24.8
	$D_{150}V_{0.4}$	85.3	27.7
	$D_{150}V_{0.5}$	90.5	29.4
4	$D_{100}V_{0.2}$	84.9	27.6
	$D_{100}V_{0.3}$	79.2	25.7
	$D_{100}V_{0.4}$	87.7	28.5
	$D_{100}V_{0.5}$	90.4	29.4

Table 5: Strain and stress in tension and compression reinforcing steel bars forbeam specimens at failure

Test series	Test beam label	Strain 10^{-3} (mm/mm)		Stress (MPa)	
		Lowe steel bars (Tension)	Upper steel bars (Compression)	Lowe steel bars (Tension)	Upper steel bars (Compression)
1	$D_{300}V_{0.0}$	3.123	0.572	570	111
2	$D_{300}V_{0.2}$	4.288	0.691	625	134
	$D_{300}V_{0.3}$	2.960	0.655	560	127
	$D_{300}V_{0.4}$	2.115	0.608	505	118
	$D_{300}V_{0.5}$	2.018	0.619	500	120
3	$D_{150}V_{0.2}$	3.050	0.655	565	127
	$D_{150}V_{0.3}$	3.103	0.686	570	133
	$D_{150}V_{0.4}$	2.966	0.670	560	130
	$D_{150}V_{0.5}$	2.614	0.660	540	128
4	$D_{100}V_{0.2}$	3.722	0.701	600	136
	$D_{100}V_{0.3}$	2.617	0.644	540	125
	$D_{100}V_{0.4}$	2.867	0.670	555	130
	$D_{100}V_{0.5}$	2.623	0.706	540	137

Note:- The yield tensile stress for the lower steel bars is 490 MPa.
- The ultimate tensile stress for the lower steel bars is 760 MPa.

3.8 Control Specimens Results

The control specimens for all beam specimens were tested at the same age of the beam specimens to measure the compressive, splitting tensile, flexural strengths and static modulus of elasticity for plain and carbon fiber concrete. Table (6) shows the results for these parameters. Generally it can be noted that there is a slight increase in the compressive strength with the increase of fiber volume fraction, also the splitting tensile, flexural strengths and static modulus of elasticity increase with the increase of fiber volume fraction. This may be due to a considerable improvement in the fiber-matrix bond [11].

Table 6: Mechanical properties of control specimens

Test series	Test beam label	Compressive Strength* (MPa)		Splitting tensile strength* (MPa)		Flexural Strength* (MPa)		Modulus of elasticity (Gpa)	
		Plain mix	FRC	Plain	Mix FRC	Plain	Mix FRC	Plain	Mix FRC
1	$D_{300}V_{0.0}$	77.3		3.8		4.0		36.2	
2	$D_{300}V_{0.2}$	----	81.4	----	4.1	----	9.1		38.0
	$D_{300}V_{0.3}$	----	81.0	----	5.5	----	9.8		38.2
	$D_{300}V_{0.4}$	----	81.9	----	5.3	----	10.2		38.7
	$D_{300}V_{0.5}$	----	82.7	----	6.0	----	10.6		39.0
3	$D_{150}V_{0.2}$	76.4	80.5	3.9	4.4	4.1	10.1	35.8	38.0
	$D_{150}V_{0.3}$	78.3	82.0	3.8	4.6	4.0	9.7	36.7	38.7
	$D_{150}V_{0.4}$	80.6	84.6	3.7	4.8	3.9	10.1	37.8	39.4
	$D_{150}V_{0.5}$	81.2	86.9	3.8	5.2	4.0	10.6	38.1	40.0
4	$D_{100}V_{0.2}$	79.9	84.1	4.1	4.6	4.3	10.3	37.5	38.8
	$D_{100}V_{0.3}$	78.7	82.5	4.2	4.7	4.4	10.5	36.9	38.7
	$D_{100}V_{0.4}$	83.5	87.7	4.5	6.2	4.8	11.2	38.4	40.4
	$D_{100}V_{0.5}$	84.2	89.3	4.6	6.1	4.9	11.8	38.8	41.1

***** The results are the average of three specimens**.**

4. Theoretical Analysis

4.1 Flexural Analysis of Fiber Reinforced Concrete Beams

The composite materials concept usually adopted to describe the mechanical behavior of FRC. The flexural strength of fiber reinforced composite material may be described as the sum of the matrix strength and fiber strength as follows:

$\sigma_{ct} = \sigma_{mt}\,\rho_m + \sigma_f\,\rho_f$ …… *(1)*

Where; σ_{ct} = Flexural strength of fiber reinforced composites in (MPa), σ_{mt} = Flexural strength of matrix in (MPa), ρ_m = Volume ratio of matrix (1- ρ_f), ρ_f = Fiber volume ratio, σ_f = Strength of fibers in (MPa).

Since the orientation, length and bonding characteristics of fibers will influence the strength of FRC; these parameters (Orientation factor α_o, Length efficiency factor α_l and Bond efficiency factor α_b of fibers) must be incorporated into equ. (1).

$\sigma_{ct} = \sigma_{mt}\,\rho_m + \alpha_o\,\alpha_l\,\alpha_b\,\sigma_f\,\rho_f$…… *(2)*

It is reasonable here to assume that the strength contribution of the concrete matrix at ultimate state may safely be neglected due to tensile cracking. So $\sigma_{mt}\,\rho_m$ In equ**.** (2) will vanished so, $\sigma_{ct} = \alpha_o\,\alpha_l\,\alpha_b\,\sigma_f\,\rho_f$…… *(3)*

Other researchers found that the bond strength between fiber and high strength concrete (HSC) is very high, this is attributed to the densification of the matrix surrounding the fibers achieved by using silica fume combination with low w/c ratio [10]. The stress in fibers reaches its ultimate strength, so the bond strength (T_f) between the matrix and fibers may be derived from the fiber ultimate strength characteristics as follows [9]:

$T_f = \sigma_{fu}\ (\frac{df}{lf})$…… *(4)*

Where, T_f is the Bond strength of fibers in (MPa), σ_{fu} is the ultimate tensile strength of fibers in (MPa), l_f is the length of fibers in (mm) and d_f is the diameter of fibers in (mm).

After substituting the parameters in equ. (4), it can be found that the fiber bond strength T_f is 4.39 MPa. **Dancygier** and **Savir** [16] who studied the flexural behavior of steel fiber concrete in low reinforcement ratios for normal and high strength concrete found that the values of fiber bond strength are taken as 2.3 MPa and 4.15 MPa for normal and high strength concrete respectively. The critical fiber length (l_c) required for breaking the fiber in the matrix is given by: $l_{ct} = \sigma_{fu}\,d_f / 2\,T_f$……*(5)*

Where l_{ct} is the critical fiber length in (mm), The composites have fiber length (l_f) of 5.5mm which exceeds the critical fiber length (l_c) 2.75mm, this confirms that the fibers will break before pulling out from the matrix. The ultimate strength σ_t of fiber reinforced concrete is:

$\sigma_t = \alpha_o\,\alpha_l\,\alpha_b\,\rho_f\,T_f\,(\frac{lf}{df})$…… *(6)*

Where σ_t is the ultimate strength of FRC in (MPa). The bond strength factor α_b is about 1.0 for straight fibers [17]. Let Ψ be efficiency factors for post-cracking strength ($\alpha_o \times \alpha_l$) allowing for both fiber length and fiber orientation which can be calculated as following [9]:

$\Psi = \frac{1}{5}(1 - \frac{5\,lct}{7\,lf})$ *for* $l_f \geq \frac{10}{7}\,l_{ct}$…… *(7)*

After substituting the l_f and l_{ct} in above equ., the value of Ψ will be 0.129. Finally equ. (6) becomes, $\sigma_t = 0.129\,\rho_f\,T\,(\frac{lf}{df})$…… *(8)*

The ultimate strength σ_t of a FRC may now be employed to derive the flexural capacity of reinforced concrete beams containing CF. Figures (19) and (20) show the strain and stress distribution of plain and FRC beams respectively. Figure (20-D) shows a stress block of fiber concrete composite after cracking, where for plain concrete (without fibers) the tensile strength of concrete will be neglected as shown in Figure (19-D), but for FRC the fibers are extending at constant load across a crack throughout the tensile section. The ultimate post-cracking tensile strength of the composite σ_t will be calculated from equ. (8).

4.2 Flexural Analysis of Doubly Reinforced Plain Concrete Beams

For Figure (19-D), since the compression reinforcing bars do not yield when the doubly reinforced beam fails in flexural (over reinforcement), so the neutral-axis depth c can be derived from the equilibrium condition in the cross section [18], $c = \frac{As\,\sigma y - A's\,\sigma's}{\gamma f'c\,\beta 1\,b}$…… *(9)*

Where; c = Neutral axis depth in (mm), A_s = Area of tensile steel bars in (mm^2), σ_y = Yield strength of tensile reinforcement bar in (MPa), A'_s = Area of compression steel bars in (mm^2), σ'_s = Strength of compression reinforcement bar at beam failure in (MPa),
b = Width of beam cross section in (mm), h = Height of beam cross section in (mm),
γ = Concrete stress block parameter (equal to 0.86 for $f'c \geq 55$ MPa), f'_c = Compressive strengthof plain concrete in (MPa), β_1 = Concrete stress block parameter (equal to 0.65 for $f'c \geq 55$ MPa).

The nominal flexural strength of over reinforced doubly reinforced plain concrete beams (ACI 318M-08) is derived as follows [18]: $M_n=(A_s\sigma_y - A'_s\sigma'_s)(d - \frac{a}{2})+A'_s\sigma'_s(d - d')$ ……. *(10)*

Where; M_n = Nominal moment capacity in (KN.m), a =Depth of rectangle compressive stress (equal to $\beta_1 c$), d = Distance from extreme compression to centroid of tension steel bars in (mm), d'=Distance from extreme compression to centroid of compression steel bars in (mm).

4.3 Flexural Analysis of Full Depth Fiber Reinforced Concrete Beams

From Figure (20a.D), the neutral-axis depth c can be derived from the equilibrium condition in the cross section, $c= \frac{(As\,\sigma y - A's\,\sigma' s) + \sigma tbh}{\gamma f'cf\beta 1b + \sigma tb}$ …… *(11)*

Where; f'_{cf} is the compressive strength of fibrous concrete in (MPa).

The nominal flexural strength of over reinforced doubly reinforced concrete beams containing carbon fibers at full depth of cross section is derived as follows:

$M_n = (A_s\sigma_y - A'_s\sigma'_s)(d - \frac{a}{2})+A'_s\sigma'_s(d - d')+ (\frac{\sigma tb(h-c)(h+c-a)}{2})$ ……..*(12)*

4.4 Flexural Analysis of Half Depth Fiber Reinforced Concrete Beams

From Figure (20b.D), the neutral-axis depth c can be derived from the equilibrium condition in the cross section, $c= \frac{(As\,\sigma y - A's\,\sigma' s) + \sigma tbh/2}{\gamma f'c\beta 1b}$ …… *(13)*

The nominal flexural strength of over reinforced doubly reinforced concrete beams containing carbon fibers at half depth of cross section is derived as follows:

$M_n = (A_s\sigma_y - A'_s\sigma'_s)(d - \frac{a}{2})+A'_s\sigma'_s(d - d')+ (\frac{\sigma tbh(3h-2a)}{8})$ ..... *(14)*

4.5 Flexural Analysis of One-Third Depth Fiber Reinforced Concrete Beams

From Figure (20c.D), the neutral-axis depth c can be derived from the equilibrium condition in the cross section, $c= \frac{(As\,\sigma y - A's\,\sigma' s) + \sigma tbh/3}{\gamma f'c\beta 1b}$ …… *(15)*

The nominal flexural strength of over reinforced doubly reinforced concrete beams containing carbon fibers at one third depth of cross section is derived as follows:

$M_n = (A_s\sigma_y - A'_s\sigma'_s)(d - \frac{a}{2})+A'_s\sigma'_s(d - d')+ (\frac{\sigma tbh(5h-3a)}{18})$ …… *(16)*

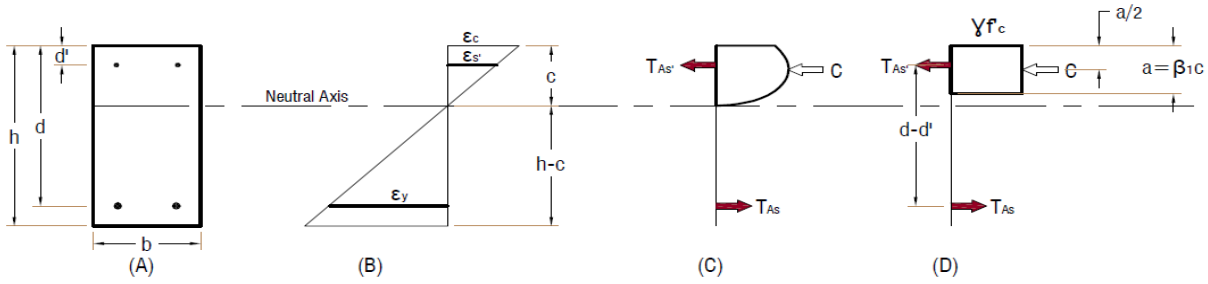

Fig.19: Strain and stress distribution for the cross section of doubly reinforced plain concrete beam (ACI 318M-08)

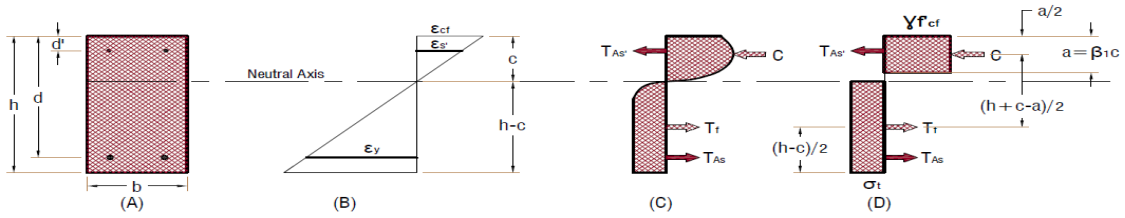

(a) Full depth fiber inclusion

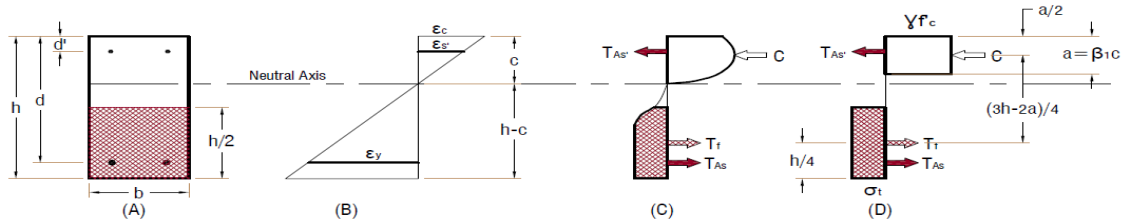

(b) Half depth fiber inclusion

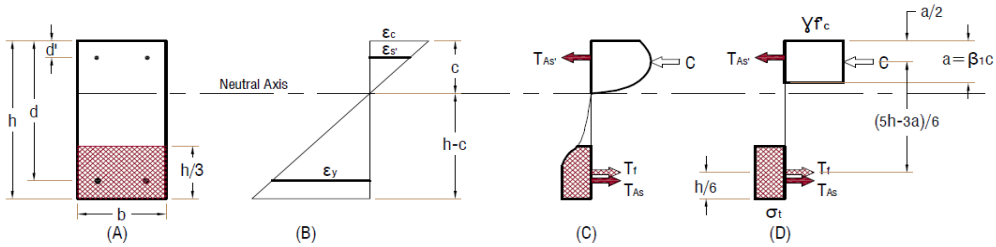

(c) One-third depth fiber inclusion

Fig.20: Strain and stress distribution for the cross section of conventional reinforced fiber concrete beams

4.6 Flexural Analysis of Full Depth Fiber Reinforced Concrete Beams According to the ACI 544 Committee

This method has been developed for predicting the strength of beams reinforced with both bars and steel fibers and applicable only when the fibers distributed in overall cross section with an aspect ratio less than 100. It is similar to ACI ultimate strength design method. The tensile strength computed for the fibrous concrete is added to that contributed by the reinforced bars to obtain the ultimate moment [19].

$$M_n = (A_s\sigma_y - A'_s\sigma'_s)(d - \frac{a}{2}) + A'_s\sigma'_s(d - d') + (\frac{\sigma t b(h-e)(h+e-a)}{2}) \quad \ldots\ldots\ldots\ldots\ldots (17)$$

$$e = (\varepsilon_y + 0.003)\frac{c}{0.003} \quad \ldots\ldots\ldots\ldots\ldots (18)$$

$$\sigma_t = 0.00772\ \alpha_b\ \rho_f\ (\frac{lf}{df}) \quad \ldots\ldots\ldots\ldots\ldots (19)$$

Where e is the distance from extreme compression fiber to top of tensile stress block of fibrous concrete in (mm), ε_y is the tensile strain in tension steel bars at theoretical moment strength of beam (Table 5). In this analysis the maximum usable strain at the extreme concrete compression fiber is taken to be 0.003. As mentioned before, the bond strength factor α_b is about 1.0 for straight fibers. Note, though, that the expression of the fibrous concrete stress in Eq.(19) (with the coefficient 0.00772) incorporates 2.3 MPa bond strength of normal strength concrete. Assuming that, an average, pullout is half of the fiber's length. According to this model, the fibrous concrete tensile stresses are uniformly distributed over an area with a height of (h-e). The basic assumptions are shown in Fig.(21).

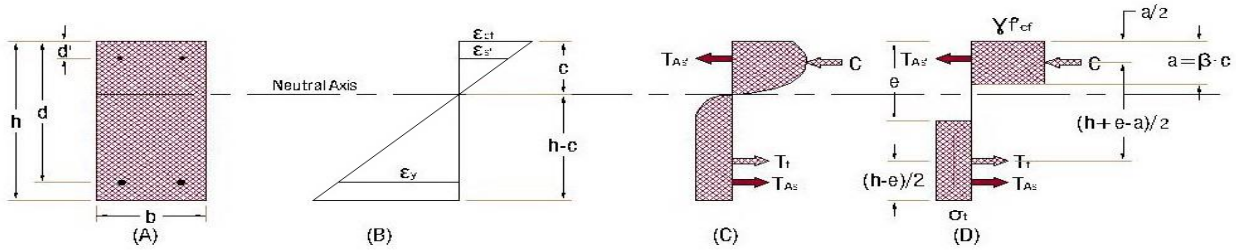

Fig. 21: Strain and stress distribution for cross section of conventional reinforced fiber concrete beams (ACI 544.4R-88)

4.7 Theoretical Results and Discussion

The required data (A_s, A_s', σ_y, σ'_s, f'_c, f'_{cf} and ε_y) are taken from Tables (1), (4) and (5), then they were substituted in the Equations (9) to (19) to analyze the moment capacity of conventional reinforced concrete beams containing different volume fractions of CF with full, half and one-third fiber depth inclusion. Table (7) shows the experimental and calculated moments for beam specimens used in this investigation and it can be seen that, for the specimen that did not include fibers, these models yield the same prediction. Table (7) also indicates that both the conventional flexural theory ACI 318M-08 model (without considering fibers) and The ACI 544 model (which is applicable only for full depth steel fiber inclusion with aspect ratio less than 100 and developed for normal strength concrete

instead of high strength concrete [19]) considerably underestimates the ultimate flexural capacity of fiber reinforced beams.. It can be concluded from this comparison that FRC theory can be employed to analyze the flexural behavior of reinforced concrete beams containing chopped CF at different depth fiber inclusion.

Table 7: Measured and calculated ultimate moment capacity for beam specimens

Test series	Test beam label	Experimental failure moment (Measured) (KN.m)	Ultimate tensile strength FRC (MPa)	Ultimate tensile strength FRC (MPa) (ACI 544.4R)	Calculated moment (KN.m)			Ratio Cal./Exp. Moments		
					Without considering fibers (ACI 318M)	With considering fibers	With considering fibers (ACI 544.4R)	Without considering fibers (ACI 318M)	With considering fibers	With considering fibers (ACI 544.4R)
1	$D_{300}V_{0.0}$	38.35	----	----	33.13	33.13	33.13	0.864	0.864	0.864
2	$D_{300}V_{0.2}$	42.90	0.89	0.12	36.27	41.65	37.03	0.845	0.971	0.863
	$D_{300}V_{0.3}$	41.28	1.33	0.18	32.56	40.66	33.73	0.789	0.985	0.817
	$D_{300}V_{0.4}$	40.95	1.78	0.24	29.42	40.25	30.99	0.719	0.983	0.757
	$D_{300}V_{0.5}$	43.55	2.22	0.30	29.14	42.60	31.10	0.669	0.978	0.714
3	$D_{150}V_{0.2}$	38.68	0.89	----	32.80	37.02	----	0.848	0.957	----
	$D_{150}V_{0.3}$	41.60	1.33	----	33.10	39.41	----	0.796	0.947	----
	$D_{150}V_{0.4}$	42.58	1.78	----	32.55	40.98	----	0.764	0.962	----
	$D_{150}V_{0.5}$	43.88	2.22	----	31.41	41.94	----	0.716	0.956	----
4	$D_{100}V_{0.2}$	43.55	0.89	----	34.82	37.97	----	0.800	0.872	----
	$D_{100}V_{0.3}$	40.63	1.33	----	31.40	36.13	----	0.773	0.889	----
	$D_{100}V_{0.4}$	42.25	1.78	----	32.29	38.61	----	0.764	0.914	----
	$D_{100}V_{0.5}$	43.23	2.22	----	31.42	39.32	----	0.727	0.910	----

5. Conclusions

From the experimental results and theoretical analysis presented in this investigation, the following conclusions can be drawn:

1. For a specific fiber volume fraction, the load-deflection patterns for partial depth fiber inclusion are practically similar to those of the corresponding full depth fiber reinforced beams. So it can be concluded that partial depth inclusion of fiber can be used in more efficient and economical manner.

2. The addition of CF causes a considerable increase in the first crack load, the percentage increase for full depth fiber inclusion is between 80-105%, while there is a slight increase in ultimate load between 7-14% relative to the plain concrete beam.

3. The resilience of beam specimens containing CF significantly increases in comparison with the reference beam specimen (without fibers). The resilience increases as the fiber volume fraction increases.

4. The resilience of beam specimens with full depth fiber inclusion is more than that with partial depth fiber inclusion; the percentage increase in resilience for beams with fiber

volume fraction 0.4% is about 270%, 101% and 40% for full, half and one-third depth of fiber inclusion respectively relative to the reference beam.

5. Both models (ACI 318M-08 and ACI 544.4R-88) considerably underestimate ultimate flexural capacity of fiber reinforced beams. According to ACI 318M and ACI 544.4R models the average ratios of calculated to measured moment for beams with full depth of fiber are 0.775 and 0.803 respectively.
6. The contribution of ultimate tensile strength of FRC matrix with ultimate moment capacity of conventional steel reinforced beams makes the analysis more realistic and close with measured moment capacity. The average ratios of calculated to measured moment for conventional reinforced beams with full, half and one-third fiber depths are 0.979, 0.956 and 0.896 respectively.

6. References

[1] Rashid, M. A., Mansur, M. A. M. and Paramecium, P., "Correlations Between Mechanical Properties of High-Strength Concrete", *Journal of Materials in Civil Engineering (ASCE)*, Vol. 14, No. 3, June, 2002, PP. 230-238.

[2] Ashour, S. A. and Wafa, F. F., "Use of Steel Fiber as Shear Reinforced in High Strength Concrete Beams", *Proceeding of the Fourth International Symposium on Fiber Reinforced Cement and Concrete*, Sheffield, 1992, PP. 517-529.

[3] Victor, C. LI., "Large Volume, High-Performance Applications of Fiber in Civil Engineering", *Journal of Applied Polymer Science*, Vol. 83, 2002, PP. 660-686.

[4] Chen, P. W and Chung, D. D. L., "Cement Reinforced with Up to 0.2 vol.% of Short Carbon Fibers", *Composites*, Vol. 24, No. 1, 1995, PP. 33-52.

[5] Chen, P. W. and Chung, D. D. L., "Low-Drying-Shrinkage Concrete Containing Carbon Fiber", *Composites*, Part B 27B, 1996, PP. 269-274.

[6] Khalil, W. I. , "Mechanical Properties of High Performance Carbon Fiber Concrete", accepted in *Engineering and Technology Journal*, 2011.

[7] ACI 318M-08 ,"Building Code Requirements for Structural Concrete (ACI 318M-08) and Commentary", *An ACI Standard, Reported By ACI Committee 318*, 2008.

[8] Raouf, Z. A., "Dynamic Mechanical Properties of Fiber-Reinforced Cement Composites", *Ph. D. Thesis, University of Manchester*, May, 1975.

[9] Hannant, D. J., "Fiber Cements and Fiber Concrete", A Wiley-Interscience Publication. 1978.

[10] Katz, A., Li, V. C. and Kazmer, A., "Bond Properties of Carbon Fibers in Cementitious matrix", *Journal of Materials in Civil Engineering (ASCE)*, Vol. 7, No. 2, May, 1995, PP. 125-128.

[11] Johnston, C. D., "Fiber-Reinforced Cement and Concrete", *Advance in Concrete technology*, Vol. 3, 2006, PP. 185-187.

[12] Dwarakanath, H. V. and Nagaraj, T. S., "Deformational Behavior of Reinforced Fiber Reinforced Concrete Beams in Bending", *Journal of Structural Engineering (ASCE)*, Vol. 118, No. 10, October, 1992, PP. 2691-2698.

[13] Padmaragaiah, S. K. and Ramaswamy A., "Comparative Study on Flexural Response of Full and Partial Depth Fiber-Reinforced High Strength Concrete", *Journal of Materials in Civil Engineering (ASCE)*, Vol. 14, No. 2, April 1, 2002, PP. 130-136.

[14] Naaman, A. E. And Reinhardt, H. W., "High Performance Fiber Reinforced Cement Composites 2 (HPFRCC 2)", Proceeding *of the Second International RILEM Workshop*, First Edition, 1996.

[15] Si-Larbi, A., Ferrier, E. and Hamelin, P., "Flexural Behavior of MRBC Beams (Multi-Reinforcing Bars Concrete Beams), Promoting the Use of FRHPC", *Composite structures*, 2006, PP. 163-174.

[16] Dancygier, A. N. and Savir Z. "Flexural Behavior of HSFRC with Low Reinforcement Ratios", Engineering *Structures*, Vol.28, 2006, PP.1503-1512.

[17] Oh, B. H. and Member, ASCE, "Flexural Analysis of Reinforced Concrete Beams Containing Steel Fibers", *Journal of Structural Engineering (ASCE)*, Vol. 118, No. 10, October, 1992, PP. 2821-2836.

[18] Nilson, A. H., Darwin, D. and Dolan and Ch. W., "Design of Concrete Structures", Thirteenth Edition, International Edition 2003.

[19] ACI Committee 544 "Design Considerations for Steel Fiber Reinforced Concrete", ACI 544.4R-88, American Concrete Institute, 1988, Reapproved 1999.